

# QUASI-MONOCHROMATIC POSITRONS USING DIPOLE AND WEDGE\*

R. Abrams#, C. Ankenbrandt and C. Yoshikawa

Muons, Inc., Batavia, IL, 60510, USA.

## Abstract

Positrons produced by electrons impinging on a target cover a broad momentum range. By bending the positrons  $180^\circ$  in a dipole magnetic field, the momenta are dispersed along the exit plane of the magnet. A wedge-shaped absorber placed at the exit plane can reduce the momenta accordingly to produce a quasi-monochromatic beam of positrons. Simulation results are presented for 2, 5, and 10 MeV/c quasi-monochromatic positrons produced by 75 MeV electrons on a tungsten target.

## CONCEPT

The method is based on 1) dispersion of the momenta by the magnet and 2) using a wedge to provide progressive momentum loss to reduce the momenta after the wedge to a common value.

The dipole and wedge layout for a simulated [1] idealized positron beam consisting of 4 discrete momenta at normal incidence is shown in Figure 1.

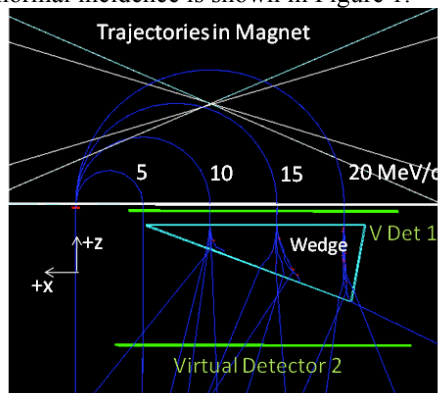


Figure 1: Dipole magnet and wedge with beam entering at left and 4 discrete beam momenta emerging at right. Trajectories for 5 - 20 MeV/c positrons emerging from dipole and wedge with  $\sim 5$  MeV/c momentum.

The trajectories are semi-circular and emerge as 4 separate beams. The figure shows trajectories for 5 beam particles at each momentum. The wedge shown is Be and is designed to reduce all of the incoming momenta to 5 MeV/c, a quasi-monochromatic beam. Scattering of the positrons in the wedge is as indicated.

\*This work was funded by Pacific Northwest National Laboratory which is operated for the U.S. Department of Energy by Battelle Memorial Institute under Contract DE-AC06-76RLO 1830.

# boba247@muonsinc.com

When the incident positrons are not normal to the magnet, their trajectories appear to be grouped near the normal incidence trajectory, but not to a single point, as shown in Figure 2. Restricting the initial positron angle reduces the spread in outgoing positrons.

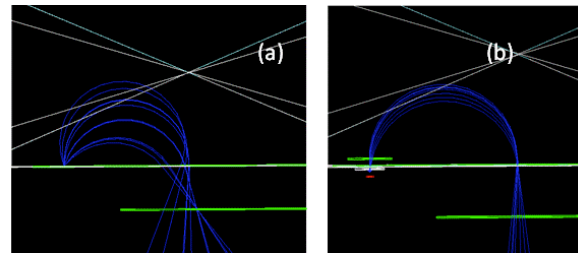


Figure 2: Trajectories for positrons originating with  $\sigma(\tan(\Theta_{\text{init}})) = 0.8$  Gaussian angular spread (a) unlimited; (b)  $\tan(\Theta_{\text{init}})$  limited to  $\pm 0.2$ , i.e.  $\Theta_{\text{init}} \leq \pm 11.2^\circ$ .

The relation between initial angle and position after the magnet is shown in Figure 3. The maximum displacement of the positron occurs for normal incidence to the magnet. For other angles there is smaller displacement, similar to the range of a projectile peaking around  $45^\circ$  initial angle.

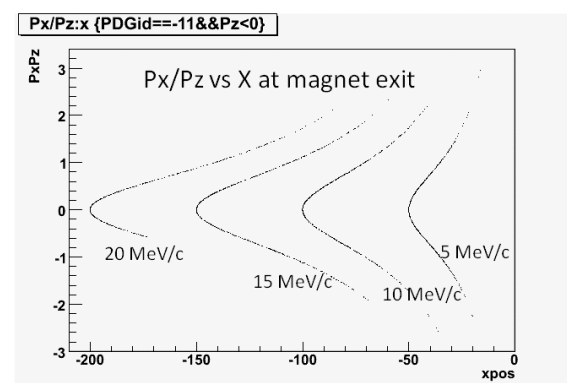


Figure 3: Tangent of initial positron angle ( $\Theta_{\text{init}}$ ) in bend plane vs. displacement at exit from magnet. Data points were generated from a Gaussian distribution with RMS = 0.8 in the tangent of the incident angle.

One can see in Figure 3 that the correlation between momentum and position depends on the range of initial angles, but with good separation for the dispersed momenta shown.

## DESIGN OF WEDGES

Design of the wedges for this study was done by simulating the momentum loss and scattering for positrons in the momentum range of interest, and matching the thickness and length of the wedge to the desired final momenta and the range of momenta impinging on the wedge.

### Wedge Materials

In general, low-Z materials produce less scattering for a given energy loss. Three materials were considered: liquid hydrogen (LH2), lithium hydride (LiH), and beryllium (Be). The results showed that LH2 produces significantly less scattering than either LiH or Be, and somewhat smaller RMS spreads in momentum loss, but the thickness required is 4 to 10 times as large, and the complications of using LH2 make it less practical. Differences between LiH and Be are less marked. Detailed results for Be are presented in the remainder of this paper.

### Design of Be Wedge for 5 MeV/c Final Momenta

The layout of the simulations is shown in Figure 1. The magnetic field region is 350mm x150mm, with a 50mm gap. The iron yoke is 500mm x 150mm, and 150mm high. The magnetic field is 0.667T and uniform. The radii are 25mm for 5 MeV/c, 50mm for 10 MeV/c, etc. The Be wedge is 58mm thick and 160mm long. In Figure 1 there were 4 positrons generated at each momentum.

The results for the positrons emerging from the wedge are shown in Figure 4.

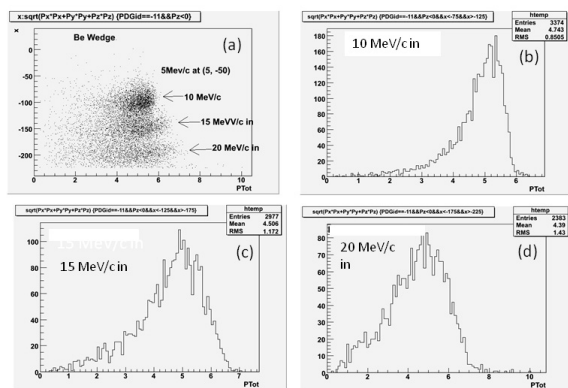


Figure 4: Results of 5MeV/c Be wedge calibration; (a) x-position vs. momentum for 5, 10, 15, and 20 MeV/c initial momenta, (b), (c) and (d) momentum distributions after the wedge for 10, 15, and 20 MeV/c initial momenta, respectively.

Figure 4(a) is a scatter plot of position vs. momentum, which shows bands in x and momentum. By selecting bands in x one can isolate and measure the component momentum distributions after the wedge. The resulting momentum distributions, in Figures 4 (b), (c), and (d),

show that the 15 and 20 MeV/c distributions are somewhat broader than that of 10 MeV/c, due to passing through more material to be degraded to 5 MeV/c.

### Design of Be Wedges for 2 MeV/c and 10 MeV/c Final Momenta

Similar procedures were used to create appropriate wedges for 2 MeV/c and 10 MeV/c final momenta. All wedges were the same length, 160mm, and the magnetic field was scaled to place the desired momentum at the same x-position.

## RESULTS FOR POSITRON SAMPLE AS PRODUCED BY 75 MeV ELECTRONS ON TUNGSTEN TARGET

### Results for 5 MeV/c Wedge

To test the dipole and wedge performance with a more realistic sample of positrons, a simulation of the production of positrons by 75 MeV/c electrons on a 4.4mm W target was performed [2] using G4beamline. A set of positrons was generated by  $1 \times 10^6$  electrons. The configuration is shown in Figure 5. Shielding blocks were added to reduce the number of stray particles that hit the virtual detector (green).

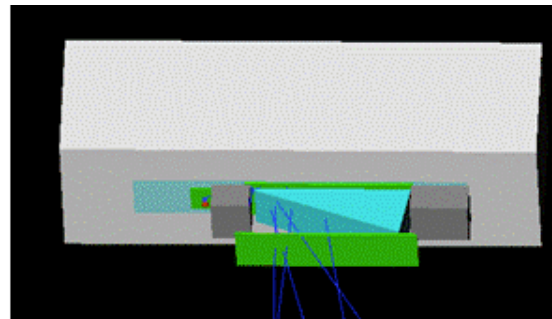


Figure 5: Test Layout; Dipole and Wedge; Pb shielding blocks along magnet gap are in dark grey, virtual detectors are in green, beam tracks originate at red dot.

Results for the momentum spectra using the 5 MeV/c wedge are shown in Figure 6. The initial momentum distribution is in Figure 6(a) and the final momentum distribution is shown in Figure 6(b). The resultant distribution has FWHM of 1 MeV/c, or an RMS spread of 0.4 MeV/c, or 8%.

Plots of x-position versus momentum and angle distributions before and after the wedge are shown in Figure 7. Figure 7(b) shows how the final distribution is improved by the wedge. The distribution in angle in the x-z plane is also sharpened after the wedge, as shown in Figure 7(c) and 7(d), which is due to absorption of the low- and high-momenta in the shielding blocks that are placed on either side of the wedge, as well as absorption in the wedge. The FWHM is 30°, which corresponds to an RMS angle of 14°.

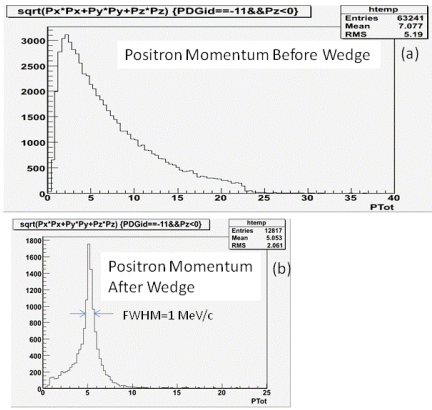


Figure 6: Momentum spectra of positrons before (a) and after (b) 5 MeV/c wedge.

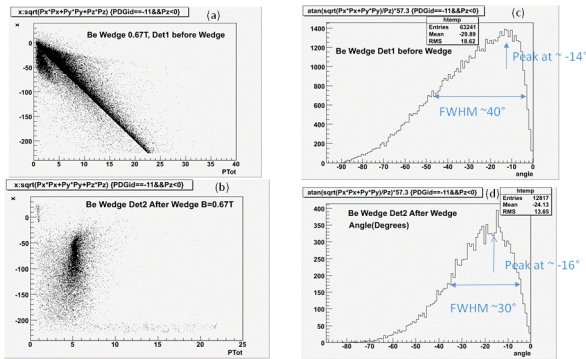


Figure 7: Scatter plot of x-position vs momentum before (a) and after (b) wedge; angle distribution before (c) and after (d) wedge.

*Summary of Results for 2, 5, and 10 MeV/c Final Momenta*

Similar computations were performed with wedges designed to produce 2 MeV/c and 10 MeV/c momenta. Results are shown in Table 1. The momentum peak sharpens with increasing momentum, and the angular spread is nearly independent of momentum.

Table 1: Momentum Peak, Angle, and Number of Surviving Positrons for 2, 5, and 10 MeV/c for Wedge

P <sub>Final</sub> (MeV/c)	P <sub>RMS</sub> /P <sub>Final</sub> (%)	θ <sub>RMS</sub> (°)	# e <sup>+</sup> After Wedge (Y <sub>Wedge</sub> )
2	15	17	2961
5	8	18	12180
10	4	19	8725

**EFFECTS OF CUTS ON POSITRON PRODUCTION ANGLE**

The results of applying cuts to the tangent of the angle in the x-z plane are shown in Figure . The momentum distributions and the angle distributions become narrower as the cuts are made more restrictive. A summary of the results is shown in Table 2.

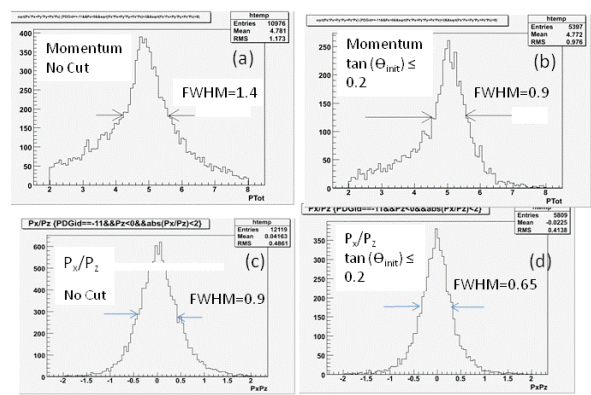


Figure 8: Momentum distributions after wedge for (a) no cut, (b)  $\tan(\theta_{init}) \leq 0.2$ ;  $\tan(\theta_{final})$  distributions for (c) no cut, (d)  $\tan(\theta_{init}) \leq 0.2$ .

Table 2: Effect of Limiting Initial Positron on Number and Characteristics of Positrons

	All $\tan(\theta_{init})$	$\tan(\theta_{init}) \leq 0.5$	$\tan(\theta_{init}) \leq 0.2$
#e <sup>+</sup> before wedge	34570	24793	13885
#e <sup>+</sup> after wedge	12180	10092	5832
P <sub>tot</sub> (FWHM)	1.4 MeV/c	1.1 MeV/c	0.9 MeV/c
P <sub>x</sub> /P <sub>z</sub> (FWHM)	0.9	0.85	0.65

**USE OF COLLIMATOR INSTEAD OF WEDGE**

The results of a simulation using a collimator instead of a wedge are shown in Table 3. With similar momentum widths and angular spreads the wedge yields ~4 to 8 times as many positrons as the collimator.

Table 3: Results for Collimator, Y is Positron Yield

P <sub>Final</sub> (MeV/c)	P <sub>RMS</sub> /P <sub>Final</sub> (%)	θ <sub>RMS</sub> (°)	#e <sup>+</sup> After Coll	Y <sub>Wedge</sub> /Y <sub>Coll</sub>
2	13	15.5	442	6.7
5	10	14.8	1424	8.3
10	4.5	12.7	2459	3.6

**CONCLUSIONS**

A dipole and wedge is shown to yield ~4 to 8 times more quasi-monochromatic positrons than a comparable resolution dipole and collimator spectrometer without significantly degrading the angular spreads.

**REFERENCES**

[1] All of the simulations in this paper were done with G4beamline, a GEANT4-based simulation package, available at <http://g4beamline.muonsinc.com>.  
 [2] C. Yoshikawa, et al, contribution #MOPEA043 at IPAC2010, May, 23-28,2010, Kyoto, Japan.